Decentralized Grid-Forming Control Strategy and Dynamic Characteristics Analysis of High-Penetration Wind Power Microgrids

Zhuoli Zhao, *Member, IEEE,* Xi Luo, Jindian Xie, Shaoqing Gong, Juntao Guo, Qiang Ni, Chun Sing Lai, *Senior Member, IEEE*, Ping Yang, Loi Lei Lai, *Life Fellow, IEEE,* and Josep M. Guerrero, *Fellow, IEEE*

***Abstract*—As wind power generation transitions from centralized development mode to decentralized on-site consumption mode, microgrid (MG) can provide an efficient solution for wind power integration into the distribution network. However, the high-penetration wind power MG is the typical weak power grid system. The traditional wind turbine generator (WTG) participates in system frequency regulation through grid-following current source, which relies on the phase-locked loop for voltage phase synchronization and is unable to provide strong frequency support in weak power grid conditions. To fill this gap, this paper presents a decentralized grid-forming control strategy of high-penetration wind power MG. A wind power adaptive dynamic droop mechanism considering wind energy characteristics and rotor speed dynamic is proposed, cooperating with the implementation of wind maximum power point tracking (MPPT) for economical operation. A detailed small-signal model for voltage source wind power-based system considering electromechanical transients and adaptive droop mechanism is developed. The dominant modes are figured out and the critical control parameters are established and optimized. The proposed wind power adaptive droop mechanism can effectively provide frequency regulation and robust control performance. Theoretical analysis, time-domain simulation results and hardware-in-the-loop experiments under various scenarios verify the feasibility and effectiveness of the proposed strategy.**

***Index Terms*—Microgrids, DFIG, grid-forming, adaptive droop, voltage source, small-signal model, dynamic characteristics analysis.**

This work was supported by the National Natural Science Foundation of China 51907031; Guangdong Basic and Applied Basic Research Foundation (Guangdong-Guangxi Joint Foundation) 2021A1515410009; Department of Education of Guangdong Province: New and Integrated Energy System Theory and Technology Research Group 2016KCXTD022; VILLUM FONDEN under the VILLUM Investigator Grant (no. 25920): Center for Research on Microgrids (CROM). (Corresponding authors: Qiang Ni; Loi Lei Lai)

Z. Zhao, X. Luo, J. Xie, S. Gong, J. Guo, Q. Ni, and L. L. Lai are with the Department of Electrical Engineering, School of Automation, Guangdong University of Technology, Guangzhou, 510006, China (e-mail: zhuoli.zhao@gdut.edu.cn; rossellaw@foxmail.com; 1446939606@qq.com; shaoqing_gong@163.com; jt_guo22@163.com; nq666@gdut.edu.cn; l.l.lai@ieee.org).

C. S. Lai is with Brunel Interdisciplinary Power Systems Research Centre, Department of Electronic & Electrical Engineering, Brunel University London, London, UB8 3PH, UK and also with the Department of Electrical Engineering, School of Automation, Guangdong University of Technology, Guangzhou, 510006, China (e-mail: chunsing.lai@brunel.ac.uk).

P. Yang is with the Guangdong Key Laboratory of Clean Energy Technology, South China University of Technology, Guangzhou 510640, China (e-mail: eppyang@scut.edu.cn).

J. M. Guerrero is with the Department of Energy Technology, Aalborg University, 9220 Aalborg, Denmark (e-mail: joz@energy.aau.dk).

I. Introduction

At present, there is an increasing proportion of renewable energy (RE) especially wind power generation due to the economic and low-carbon advantages. RE has been connected to the distribution network on a large scale. Microgrids (MGs) have the natural advantages of independence and flexibility compared with the conventional centralized distribution network, providing an effective solution for the access of RE. It is foreseeable that there will be more and more MGs with high penetration of RE generation, which will form the embryonic form of the future smart grid [1]-[2]. However, wind power generation suffers from high level of power variability and unpredictable nature [3]. As the penetration of wind power generation increase to a high level, the intermittent nature becomes a more significant problem as the limited capability of balancing the power in the system. As a result, there is an urgent need to make them controllable and can be guaranteed for the high penetration RE microgrid system [4]-[5].

New and severe challenges emerge when wind power becomes high penetration. Most of the traditional wind power is designed in MPPT mode through the power converter to deliver power to the public grid. Fixed voltage and frequency from the strong grid are necessary to the traditional wind turbine generator (WTG) which can be represented by an ideal grid-following current source. The converter control system decouples the power side from the system frequency and the WTG will not respond to the grid frequency [6]. Since the converter hides the rotational kinetic energy of the generator, current-source WTG is hardly to provide continuous and effective active power support as well as frequency regulation for the MG system.

A. The Review of Literature

1) Traditional Wind Turbine Generators Participate in System Frequency Regulation

Recently, some literature has been reported to study the WTG participating in system frequency regulation through grid-following current source approach, which can be mainly classified into three categories: retaining power reserve [7]-[10], simulating virtual inertia [11]-[13], equipping dispatchable power generation units [14]-[17].

In [7], a modified MPPT curve is proposed to establish the power reserve, which enables the active power output of WTGs reserved instead of tracking the maximum power point. WTGs can adjust the output power during frequency excursion events by deloading operation. In [8], the overspeed and pitch angle control method are proposed for deloading operation to take part in the primary frequency regulation. Combining variable droop coefficient and overspeed control of WTGs, primary frequency regulation and inertial response strategy are proposed in [9] and [10], which has the ability of frequency support in the case of wind speed fluctuations. However, the method of retaining power reserve essentially responds to the system frequency by adjusting the active power rather than directly participate in frequency response.

The other kind of method is to simulate the rotation characteristics of traditional generators in order to deal with the lack of physical inertia in wind power system. In [11]-[13], the proposed virtual inertia strategy can emulate the behavior of synchronous generators in frequency excursion events. In [12], an improved current-controlled virtual synchronous generator (VSG) strategy for wind power system is proposed. However, virtual inertia cannot directly participate in long-term frequency adjustment and it is only suitable for suppressing rapid frequency changes caused by load disturbances in the system. When the rotor speed changes, the rotor kinetic energy will lose adjustment ability which adjustment time generally lasts for a few seconds [13].

The use of dispatchable generation units to compensate for the intermittency of wind energy is also considered as a solution. Diesel generators are considered for well-performed nominal frequency restoring during intermittent wind power generation in [14] and [15]. In [16], a joint frequency regulation scheme for a wind-diesel hybrid power system is proposed, allowing excess wind energy distributed to residential consumers. Battery energy storage system (BESS) is used for mitigating the impact of intermittent wind speed on reliability to achieve frequency regulation in [17]. Even though the use of diesel generator is attractive from the reliability point of view, the dynamic response of synchronous generators is slower than inverter-based interfaces unit. On the other hand, using large-capacity batteries is extremely expensive, and how to install as small-capacity storage device as possible to the grid-following WTG has become a research problem.

2) Grid-forming Control of Wind Turbine Generators

The WTGs mentioned above can be essentially represented by an ideal grid-following current source. Most importantly, it is an urgent need to develop the grid-forming voltage source WTGs. Theoretically, the MG can provide effective solutions for voltage source mode distributed generation in RE high penetration system. PV-BESS hybrid MG autonomous systems can already operate independently in [18] and local adaptive droop control voltage-source PV system is proposed.

Recently, we conducted a study on the high-penetration wind power MG in [19] which proposed a grid-forming doubly-fed induction generators (DFIGs)-BESS hybrid stand-alone MG, enabling the DFIGs to participate in MG frequency regulation. However, the ideal grid-side converter and ideal wind turbine are considered in [19] instead of the complete modeling. In [20], a control strategy of the large-scale variable pitch and speed direct-drive permanent magnet synchronous generator (PMSG) is proposed for maintaining the voltage and power support under weak grid as well as stand-alone mode. A novel low frequency AC technique for grid-forming wind power transmission is proposed in [21]. With the small-signal stability analysis carried out, the grid-forming control strategy of PMSG also shows a good contribution to stabilize offshore grid voltage. [22] presents a synchronverter grid-forming control method implemented in the grid-side converter of PMSG, which can improve the inertial response and active power tracking performance under variable wind speed conditions.

In addition, there are some studies that apply grid-forming WTG specifically in high voltage direct current (HVDC) system [23]-[24]. The Type IV and Type III wind farm using HVDC transmission is studied in [23] and [24], respectively. The grid-forming control scheme was proposed for grid-side converter in diode rectifier-connected offshore wind farm in [23], which can limit fault current under weak grid conditions. A VSG grid-forming control scheme in DFIG-based wind power is proposed in [24]. It is revealed that VSG method has a better impedance characteristic than the regular method for DFIG. Due to the virtual inertia capability of the VSG, the DFIG wind farm is able to effectively reduce the rate of change of frequency and ensure the stability in HVDC sending-terminal system. Besides, the VSG-DFIG also has well performance in transient of voltage fault ride-through in [25].

The grid-forming WTGs mainly provide stable voltage support for remote weak grid as the sending-terminal system and it tends to operate with multiple units in fixed voltage and frequency grid-forming mode. Besides, implementing grid-forming control for each WTG is more feasible than in diode rectifier-based HVDC system because of the limited control capability of diode rectifier [23]. However, the above studies focus on the large-scale wind farm scenarios, and generally ignore the electromechanical transient dynamic and primary wind energy characteristics, which will lead to the neglect of some critical dynamics. With the increasing wind power penetration, the control strategy of grid-forming WTGs considering complete dynamics needs to be further studied under decentralized on-site consumption mode especially the autonomous mode.

3) Microgrids Stability Analysis

The stability analysis of inverter-based MGs has been extensively studied in recent years. In [26]-[27], the precise mathematical small-signal modeling of the converter-based islanded AC MG system is studied. The experiments verified the good system response performance of the droop control strategy considering phase-locked loop (PLL) in [26]. [27] compares the system modeling and stability response with and without PLL, and proposes a new small-signal modeling method based on characteristic equations to evaluate the stability of the system. Furthermore, [28] presented the detailed modeling and stability analysis of the droop control autonomous MG which shows the low-frequency oscillation mainly caused by the without-PLL droop controller. However, only the ideal BESS is considered without RE system in [26]-[28]. A detailed voltage-source PV-based MG cluster small-signal modeling

TABLE I
FUNCTION COMPARISONS BETWEEN THIS PAPER AND RELATED WORKS (Y: YES; N:NO)

Functions	[7]	[12]	[13]	[14]	[18]	[19]	[20]	[22]	[23]	[24]	[26]	[28]	[30]	This Paper
Grid-forming wind power control	N	N	N	N	N	Y	Y	Y	Y	Y	N	N	Y	Y
Wind power high-penetration	N	N	N	N	N	Y	N	N	N	N	N	N	N	Y
WTG continuous voltage support	N	N	N	N	N	Y	Y	Y	Y	Y	N	N	N	Y
WTG continuous frequency regulation	N	N	N	N	N	Y	Y	Y	Y	Y	N	N	N	Y
Microgrid autonomous operation	N	N	N	Y	Y	Y	Y	N	N	N	Y	Y	Y	Y
MPPT for WTG economical operation	Y	Y	Y	Y	Y	N	Y	Y	N	N	N	N	N	Y
Wind energy dynamic characteristics	Y	Y	Y	Y	N	N	N	N	N	N	N	N	N	Y
Rotor speed dynamic	Y	Y	Y	Y	N	N	Y	N	N	N	N	N	N	Y
Electromechanical transient dynamic	N	N	N	N	N	N	N	N	N	N	N	N	N	Y
Full-order small-signal stability analysis	N	N	N	N	Y	N	N	N	N	N	N	Y	N	Y

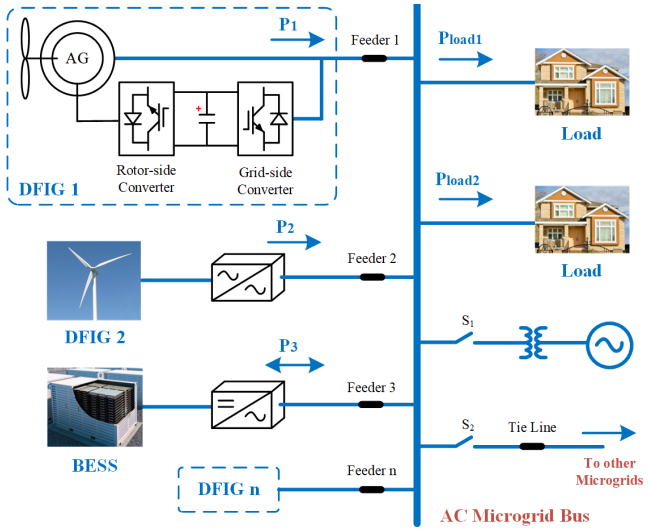

Fig. 1. System structure of the high-penetration wind power microgrid.

considering the dynamic DC link of PV is conducted in [18]. The MG cluster combining synchronous-based and inverter-based units is proposed in [29], the critical evaluation of the oscillation mode caused by the synchronous-based unit was carried out. Wind power system oscillatory stability is studied in [30], which proposes the torque and power droop-based DFIG eigenvalue sensitivity analysis. However, although the proposed strategy allows the WTG-synchronous generator MG system operates autonomously, the electromechanical transients of the WTG mechanical components and the electromagnetic transients of the inner-loop dynamics are still ignored in stability analysis, which leads to critical dynamics neglected in system. Besides, they haven't considered the full-order small-signal model of grid-forming WTG in MG thoroughly for the time being.

B. Contributions

Motivated by the aforementioned research gap, this paper proposes a decentralized control strategy of high-penetration wind power MG using DFIGs. In this scenario, wind power-based MG can be specifically applied to the islands with abundant wind energy and supply for island residents, tourism hotels, etc. As there is no strong public power grid to rely on, the DFIGs and BESS in MG should be operated as grid-forming voltage sources, providing the constant voltage for the MG system. Compared with the existing related research, more functions are taken into account in this paper which is improved in different aspects. Table I shows the comparison of this paper with existing related research. The main contributions of this paper are summarized as follows:

1) This paper proposed a decentralized grid-forming control strategy without PLL of wind power participating in frequency regulation under weak power grid conditions. By implementing complete modeling of a wind turbine, a voltage-source wind power adaptive droop (WPAD) mechanism considering primary wind energy characteristics is proposed. Cooperating with rotor speed and pitch angle control, voltage-source MPPT mode can be implemented for economical operation.

2) A comprehensive state-space model for high-penetration wind power MG considering electromechanical transients of the DFIG mechanical components and adaptive droop mechanism is developed to figure out the dominant oscillatory modes. The proposed full-order small-signal model can effectively establish and optimize the critical control parameters to enhance the stability of the system.

3) The high-penetration wind power MG is established in MATLAB/Simulink and hardware-in-the-loop (HIL) experimental environment, respectively. The time-domain simulations and experiments are performed to successfully validate the proposed strategy.

C. Paper Organization

This paper is organized as follows. Section II elaborates the architecture of the studied MG system. Section III proposes the grid-forming generation supporting control mechanism in high-penetration wind power MG. After the comprehensive control strategy presentation, the full-order small-signal model is developed and dynamic characteristics analysis is carried out in Section IV. Sections V and VI present the simulation results and HIL experiment performance under various scenarios respectively to verify the feasibility and effectiveness of the proposed strategy. Finally, the conclusion is given in Section VII.

II. SYSTEM ARCHITECTURE OF WIND POWER-BASED MICROGRIDS

At present, there are many island MGs demonstration projects in the world. Dongao Island in Guangdong, and Luxi

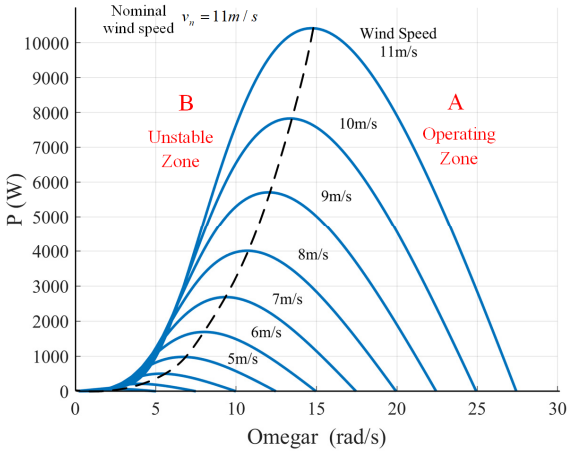

Fig. 2. Operating area analysis of wind turbine.

Island in Zhejiang, China, are all typical islanded MGs that have already operated for several years [31]-[32]. In consideration of the increasing amounts of wind power generations integrated into the MGs, Fig. 1 shows the single-line diagram and topology of the studied wind power-based MG. Since only stand-alone operation mode is considered in this work, switch S_1 and S_2 are open to isolate the utility power grid and other MGs.

As shown in Fig. 1, DFIG is chosen which are widely used in commercial onshore wind power system and have the advantages of small-capacity converter as well as low cost. Two DFIGs and one BESS are interconnected to form an islanded MG via resistive-inductive feeders for power supply to local loads. The BESS unit operates in conventional droop mode while DFIGs work in voltage-source MPPT mode for economical operation. If wind power is abundant, DFIGs can provide extra power for BESS which changes the operation mode into charging state depending on the instruction of the microgrid central controller (MGCC). It should be noted that the wind power-based sources are enabled to participate in voltage and frequency regulation and power sharing through the presented WPAD mechanism in Section III.

III. Grid-Forming Generation Supporting Control in High-Penetration Wind Power Microgrid

A. Operating Area Analysis of Grid-Forming Wind Turbine

There is an inherent power-speed characteristic operational curve of the wind turbine. Fig. 2 shows a cluster of curves of wind turbine rotating speed and the captured wind power in the situation of pitch angle equals to zero. At a fixed wind speed and fixed pitch angle, one unique curve can be determined while the operational point of wind turbine will adaptively move on the curve. Based on Equation (1), the cluster of curves can be divided into the unstable zone and operating zone, as shown in Fig. 2.

$$\frac{dP_{WT}}{d\omega_{WT}} = 0 \tag{1}$$

In Fig. 2, the highest points of all the curves (i.e., maximum power point) are connected with a dotted line, which divides the operational curves into two areas. Due to the necessary reserve power demand and deloading capacity, the wind turbine must operate in the right half zone, i.e., in the area of $dP_{WT} / d\omega_{WT} < 0$, which will be considered in Section III-B.

B. Grid-Forming Generation Supporting Control Strategy

1) Wind Power Adaptive Droop Control Mechanism

Fig. 3 presents the proposed decentralized grid-forming control strategy of DFIG in high-penetration wind power MG. In this diagram, the designed control scheme considers the primary wind power and DC voltage control for DFIG. The rotor speed controller is the crucial part of the WPAD controller in the scheme, which can achieve MPPT. In the voltage-source MPPT scheme, the operating point of the wind turbine is fixed

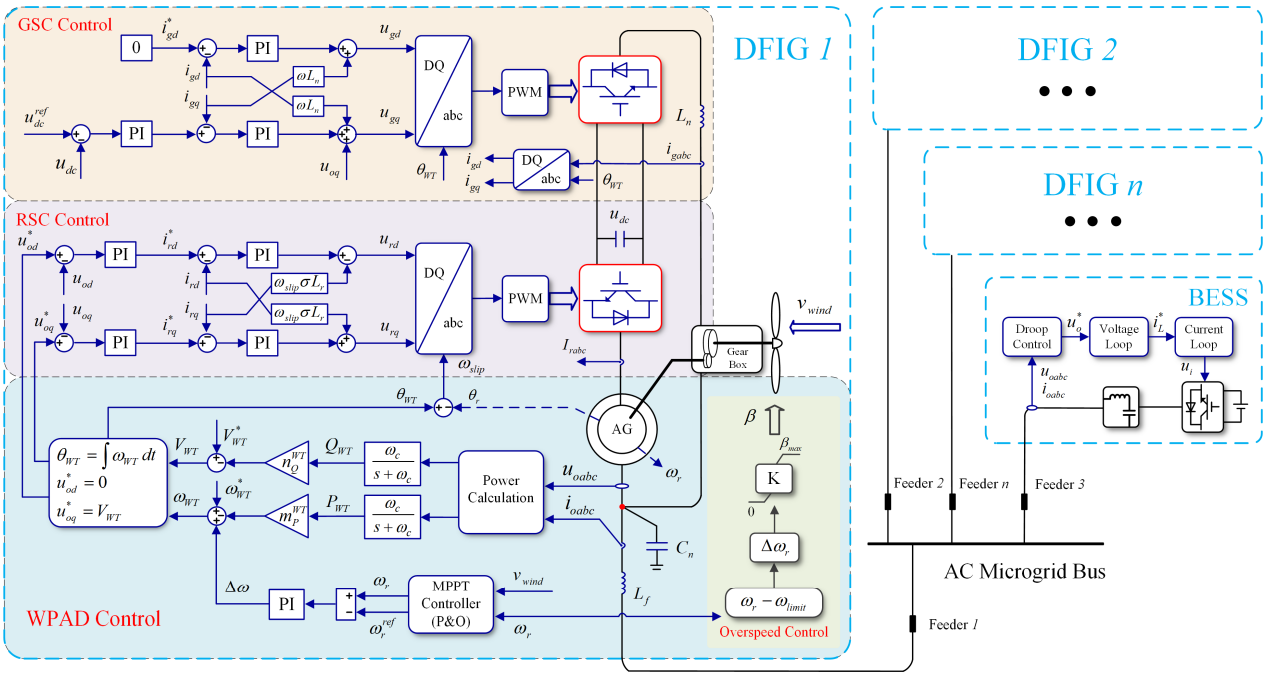

Fig. 3. Proposed decentralized grid-forming control strategy of DFIG in high-penetration wind power microgrid.

on the MPPT curve (i.e., the curve represented by Equation (1)) and the rotor speed of the wind turbine is only related to the wind speed. As the supplemental active power droop loop, the rotor speed controller is capable of adjusting the output frequency of DFIG adaptively even though load increases or wind energy decreases. The outer loop of the WPAD mechanism can be expressed as follows:

$$V_{WT} = V_{WT}^{*} - n_{Q}^{WT} Q_{WT} \tag{2}$$

$$\omega_{WT} = \omega_{WT}^{*} - m_{P}^{WT} P_{WT} + K_{pwr}(\omega_r - \omega_r^{ref}) + K_{iwr}\int(\omega_r - \omega_r^{ref})\,dt \tag{3}$$

where V_{WT}^{*} and ω_{WT}^{*} are the voltage and frequency set-value of the DFIG systems, n_{Q}^{WT} and m_{P}^{WT} are the reactive and active power droop coefficients of DFIG systems, Q_{WT} and P_{WT} are the reactive and active power of DFIG systems, K_{pwr} and K_{iwr} are the gains of rotor speed controllers, respectively.

Note that once the wind speed increases or load grows, the rotor speed will automatically increase, rotating speed can be transformed to MPP speed such that the MPPT mode is activated. Besides, the rotor speed reference value ω_r^{ref} will be updated according to the real-time wind speed, using the perturbation and observation (P&O) method, thus, ω_r^{ref} is calculated by the MPPT controller.

2) Voltage-Source Operation Mechanism

In wind power-based MG system, the DFIG studied is externally characterized as a voltage source output. It is connected to the grid through an *LCL* filter. Thus, the power circuit of DFIG can be expressed as follows:

$$\overbrace{\begin{bmatrix}\dot{i}_{odq}\\ \dot{u}_{odq}\\ \dot{i}_{gdq}\end{bmatrix}}^{\dot{x}_{PC}^{WT}} = A_{PC}\overbrace{\begin{bmatrix}i_{odq}\\ u_{odq}\\ i_{gdq}\end{bmatrix}}^{x_{PC}^{WT}} + B_{PC1}\left[u_{gdq}\right] + B_{PC2}\left[i_{sdq}\right] + B_{PC3}\left[u_{bdq}\right] + B_{PC4}\left[\omega_{WT}\right] \tag{4}$$

where i_{odq}, u_{odq}, i_{gdq}, i_{sdq} are the variables of DFIG output currents, output voltages (on capacitor), GSC output currents and output stator currents respectively. u_{bdq} are the connection point voltages in local reference frame of the DFIG system.

The back-to-back (B2B) power converters, rotor-side converter (RSC) and grid-side converter (GSC) should operate as a grid-forming voltage-source under weak grid system. The control goal of RSC maintains the amplitude and frequency of DFIG stator voltage, making sure of multiple DGs operation parallelly. GSC is to stabilize the voltage of DC bus capacitor and adjust the power factor. The modeling of RSC and GSC controller are derived with u_{odq}^{*}, u_{dc}^{*} and ω_{WT} as inputs, and u_{rdq}, u_{gdq} as outputs, which are given by:

$$\overbrace{\begin{bmatrix}\dot{\varphi}_{udq}\\ \dot{\varphi}_{idq}\end{bmatrix}}^{\dot{x}_{RSC}} = A_{RSC}\overbrace{\begin{bmatrix}\varphi_{udq}\\ \varphi_{idq}\end{bmatrix}}^{x_{RSC}} + B_{RSC1}\left[u_{odq}\right] + B_{RSC2}\left[i_{rdq}\right] + B_{RSC3}\left[u_{odq}^{*}\right] \tag{5}$$

$$\overbrace{\begin{bmatrix}\dot{\gamma}_{dc}\\ \dot{\gamma}_{idq}\\ \dot{u}_{dc}\end{bmatrix}}^{\dot{x}_{GSC}} = A_{GSC}\overbrace{\begin{bmatrix}\gamma_{dc}\\ \gamma_{idq}\\ u_{dc}\end{bmatrix}}^{x_{GSC}} + B_{GSC1}\left[u_{gdq}\right] + B_{GSC2}\left[i_{gdq}\right] + B_{GSC3}\left[u_{rdq}\right] + B_{GSC4}\left[i_{rdq}\right] \tag{6}$$

where φ_{udq}, φ_{idq} and γ_{dc}, γ_{idq} are the integrator variables of RSC and GSC controller respectively. i_{rdq} and u_{rdq} are the rotor currents and rotor voltages of DFIG. u_{dc} is the DC bus voltage.

In addition, the dynamic of DC-link which is an intermediary of power balancing between RSC and GSC can be expressed by:

$$u_{dc}C_{dc}\frac{du_{dc}}{dt} = (u_{rd}i_{rd} + u_{rq}i_{rq}) - (u_{gd}i_{gd} + u_{gq}i_{gq}) \tag{7}$$

Note that in Equations (4)-(6), the matrices A_{PC}, B_{PC}, A_{RSC}, B_{RSC}, A_{GSC} and B_{GSC} can be derived from the ODEs representing by the corresponding controllers of DFIG system.

C. Pitch Angle Overspeed Control

In some situations, the load can only consume part of captured wind energy in the autonomous system. Then as mentioned, the wind turbine will operate in the right half zone so it will adaptively find the operating point on the curve to match the load power. However, the power that wind turbine can adjust is limited when the load decreases suddenly or the wind speed is too high, which lead to the overspeed of the wind turbine. In order to prevent overspeed from damaging the turbine, an overspeed control strategy based on pitch angle is also proposed in Fig. 3, which is the auxiliary controller of the WPAD strategy. It can restrict the rotor speed within a reasonable range by increasing the pitch angle.

IV. Modeling and Stability Analysis

A. Dynamic Modeling of High-Penetration Wind Power Microgrid

The main purpose of this section is to study the small-signal ability of the high-penetration wind power MG. By combining the state-space model of the components of MG, the overall small-signal state-space model is developed completely.

Unlike most previous modeling that ignores the electromechanical transients of the mechanical components of WTGs, the detailed modeling including wind turbine and the electromagnetic transients of control system dynamics (shown in Fig. 3) are considered in this work, which is derived as follows:

1) State-Space Model of Voltage-Source DFIG

Since the voltage-source control strategy of B2B converters has been carried out in Section III-B, this section will propose the modeling of DFIG other than the control loop.

The dynamic shaft model of the wind wheel-gear-rotor and asynchronous generator (AG) can be given by:

$$\overbrace{\begin{bmatrix}\Delta\dot{\omega}_{wheel}\\ \Delta\dot{T}_m\\ \Delta\dot{\omega}_r\end{bmatrix}}^{\Delta\dot{x}_{SM}} = A_{SM}\overbrace{\begin{bmatrix}\Delta\omega_{wheel}\\ \Delta T_m\\ \Delta\omega_r\end{bmatrix}}^{\Delta x_{SM}} + B_{SM1}\left[\Delta i_{sdq}\right] + B_{SM2}\left[\Delta i_{rdq}\right] \tag{8}$$

TABLE II
SYSTEM PARAMETERS OF THE HIGH-PENETRATION WIND POWER MICROGRID

Symbol	Parameter	Value
	DFIG Unit	
P_s	Nominal Power	10kW
p	Poles of Pairs	2
v_n	Nominal Wind Speed	11m/s
R_s, L_s	Stator Resistance and Inductance	0.455Ω, 84 mH
R_r, L_r	Rotor Resistance and Inductance	0.62Ω, 85 mH
L_m	Mutual Inductance	78 mH
u_{dc}^{ref}	DC Bus Voltage	650 V
C_{dc}	DC Bus Capacitance	5 mF
L_n	Grid-side Inductance	4 mH
C_n	Output Filter Capacitance	0.03 mF
L_f	Output Filter Inductance	10 mH
K_{pwr}, K_{iwr}	Proportional and Integral Term of Rotor Speed Controller	0.015, 0.03
K_{pout}, K_{iout}	Proportional and Integral Term of RSC Controller Outer Loop	0.1, 8
K_{pin}, K_{iin}	Proportional and Integral Term of RSC Controller Inner Loop	1, 50
K_{pdc}, K_{idc}	Proportional and Integral Term of GSC Controller Outer Loop	0.3, 6
K_{pi}, K_{ii}	Proportional and Integral Term of GSC Controller Inner Loop	25, 10
	BESS Unit	
L_c	Coupling Inductance	1.35 mH
C_n	Output Filter Capacitance	0.05 mF
L_f	Output Filter Inductance	1.35 mH
K_{pv}, K_{iv}	Proportional and Integral Term of Voltage Outer Loop	0.05, 390
K_{pc}, K_{ic}	Proportional and Integral Term of Current Inner Loop	10.5, 16000
	Microgrid	
V_s	Grid Voltage	380 V
f	Nominal Frequency	50 Hz
f_{sw}	Switching Frequency	8 kHz
m_P, n_Q	Active and Reactive Power Droop Coefficient	$7.85e^{-5}$, $1.58e^{-4}$
Z_1, Z_2, Z_3	Feeder Impedance	$0.1+j0.05(\Omega)$

$$\overbrace{\begin{bmatrix}\Delta\dot{i}_{sdq}\\ \Delta\dot{i}_{rdq}\end{bmatrix}}^{\Delta\dot{x}_{AG}} = A_{AG}\overbrace{\begin{bmatrix}\Delta i_{sdq}\\ \Delta i_{rdq}\end{bmatrix}}^{\Delta x_{AG}} + B_{AG1}\left[\Delta u^{*}_{odq}\right] + B_{AG2}\left[\Delta u_{rdq}\right] + B_{AG3}\left[\Delta\omega_r\right] \quad (9)$$

In (8)-(9), $\Delta\omega_{wheel}$, ΔT_m are the state variables of rotor speed of wind wheel and output mechanical torque. $\Delta\omega_r$ is the state variable of rotor speed. Note that A_{SM}, B_{SM}, A_{AG} and B_{AG} can be derived from the ODEs representing by the shaft model and AG of DFIG.

Therefore, by transforming the control loop (Equations (2)-(6)) into a linearized small-signal model, combined with Equations (8)-(9), the state-space model of the voltage-source DFIG in synchronous reference frame is developed as follows:

$$\dot{\Delta x}_{WT} = A_{WT}\Delta x_{WT} + B_{WT}\Delta u_{bDQ} + B_{com}\Delta\omega_{com} \quad (10)$$

$$\Delta x_{WT} = [\Delta\alpha_{wr}\ \ \Delta\delta_{WT}\ \ \Delta P_{WT}\ \ \Delta Q_{WT}\ \ \Delta x_{PC}^{WT}\ \ \Delta x_{SM}\ \ \Delta x_{AG}\ \ \Delta x_{RSC}\ \ \Delta x_{GSC}]^T \quad (11)$$

In (10) and (11), $\Delta\alpha_{\omega r}$ is the integrator state of the rotor speed controller, $\Delta\delta_{WT}$, ΔP_{WT} and ΔQ_{WT} are the state variables of droop controller. Δu_{bDQ} are the connection point voltages in the synchronous reference frame of the DFIG system and $\Delta\omega_{com}$ is an additional input signal of the frequency deviation between local and synchronous reference frames.

2) State-Space Model of Network and Load Model

The dynamic model of the lines and loads in Fig. 1 can be readily constructed as follows:

$$\begin{bmatrix}\Delta\dot{i}_{line\bullet i\,DQ}\\ \Delta\dot{i}_{load\bullet k\,DQ}\end{bmatrix} = \begin{bmatrix}A_{NET}\\ A_{LOAD}\end{bmatrix}\begin{bmatrix}\Delta i_{line\bullet i\,DQ}\\ \Delta i_{load\bullet k\,DQ}\end{bmatrix} + \begin{bmatrix}B_{NET1}\\ B_{LOAD1}\end{bmatrix}\begin{bmatrix}\Delta u_{b\bullet i\,DQ}\\ \Delta u_{pccDQ}\end{bmatrix} + \begin{bmatrix}B_{NET2}\\ B_{LOAD2}\end{bmatrix}[\Delta\omega] \quad (12)$$

where $\Delta i_{line\bullet i\,DQ}$, $\Delta i_{load\bullet k\,DQ}$ are the state variables of lines and loads current respectively, $\Delta u_{b\bullet i\,DQ}$, Δu_{pccDQ} are the voltages of the connection point of the sources and the voltages of point of common coupling (i=1, 2, 3 and k=1, 2), $\Delta\omega$ represents the angular velocity corresponding to the frequency in the synchronous reference frame.

Please noted that $\Delta x_{NET} = \left[\Delta i_{line\bullet 1\,DQ}\ \Delta i_{line\bullet 2\,DQ}\ \Delta i_{line\bullet 3\,DQ}\right]^T$ and $\Delta x_{LOAD} = \left[\Delta i_{load\bullet 1\,DQ}\ \Delta i_{load\bullet 2\,DQ}\ \Delta i_{load\bullet 3\,DQ}\right]^T$.

3) State-Space Model of High-Penetration Wind Power Microgrid

As the supplementary power source in wind power-based MG, BESS also needs to perform small signal modeling. However, the grid-forming modeling of BESS represented by an ideal DC source has been carried out in [18], [28] and [33]. This section will not take it as the focus of modeling; instead, it will be interconnected with DFIGs for MG forming modeling.

The integrated dynamic model of the wind power-based MG presented in Fig. 1 can be developed as follows:

$$\dot{\Delta x}_{MG} = A_{MG}\Delta x_{MG} \quad (13)$$

$$\Delta x_{MG} = [\Delta x_{WT1}\ \ \Delta x_{WT2}\ \ \Delta x_{BESS}\ \ \Delta x_{NET}\ \ \Delta x_{LOAD}]^T \quad (14)$$

B. Stability Analysis and Design of Key Control Parameters

1) Eigenvalue Analysis of Single Voltage-Source DFIG

Firstly, this paper mainly focuses on the modeling and stability research of wind power MG, and also considers the influence of the electromechanical transient state on the system. It is necessary to carry out the investigation of the dynamic of a single DFIG through the eigenvalue analysis. The detailed parameters of the DFIG are shown in Table II. Fig. 4 shows the overview modes of single DFIG without considering the WPAD in Equation (3).

In the stand-alone single DFIG system, all the eigenvalues are located on the left plane where the real part is negative, and it means the system is stable. It can be seen that two pairs of low-frequency and a pair of ultra-low frequency eigenvalues are yielded in Fig. 4. It is worth mentioning that there is an oscillation mode with insufficient damping ratio, which is

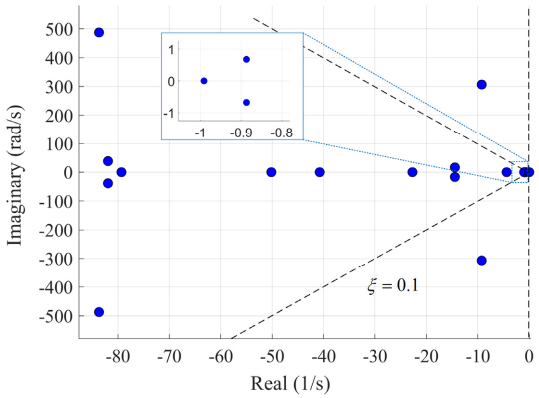

Fig. 4. Overview modes of single DFIG.

strongly associated with the state variables of Δi_{sdq} and Δi_{rdq} according to the participation factors analysis. In other words, this weakly damping oscillation mode is caused by the inherent parameters of the AG stator and rotor [34], [35].

Based on the comparison and reference with single DFIG modeling, multi-unit detailed modeling can be carried out below.

2) Eigenvalue Analysis of High-Penetration Wind Power Microgrid

The dynamic model of high-penetration wind power MG is developed in (13) and (14), which can be further adopted to evaluate the small-signal stability. The detailed parameters of the MG system are shown in Table II. It is worth mentioning that when building wind power MGs, the installed DFIG and BESS units are generally purchased from the same manufacturer and share identical system parameters. However, operations such as equipment renovation and expansion of the MGs may lead to changes in system stability due to the changes of system parameters, which needs further research about stability analysis and it is out of the scope of this paper. The dynamic characteristics analysis and the simulation of this paper are based on the mentioned premise of unified parameters.

Eigenvalue analysis enables us to determine which modes impact the response of the MG system small-signal disturbances [29], [36]. Figs. 5 (a) and (b) show the overview modes and dominant modes of the studied MG system respectively considering the WPAD control strategy. Excepting the dominant oscillation modes of the system corresponding to the dominant eigenvalues, the remaining oscillation modes can be identified as high frequency and high damping oscillation modes, which have high decay speed in the system. Therefore, only the low-frequency and ultra-low frequency modes are confirmed to be the dominant oscillation modes, which is the crucial part for stability analysis, while the influence of non-dominant modes on the system stability after disturbance can be ignored in this study.

As seen in Fig. 5 (b), eight pairs of eigenvalues are identified as the dominant modes which can stimulate system crucial oscillation responses. Several mid-low-frequency and ultra-low frequency oscillation modes yield in MG, among which two pairs of low-frequency and ultra-low frequency modes (i.e., Eigenvalue (13,14) and Eigenvalue (15,16)) match the single DFIG dominant oscillation mode. It is worth pointing out that in the usual operation of the MG, the damping ratio of all system

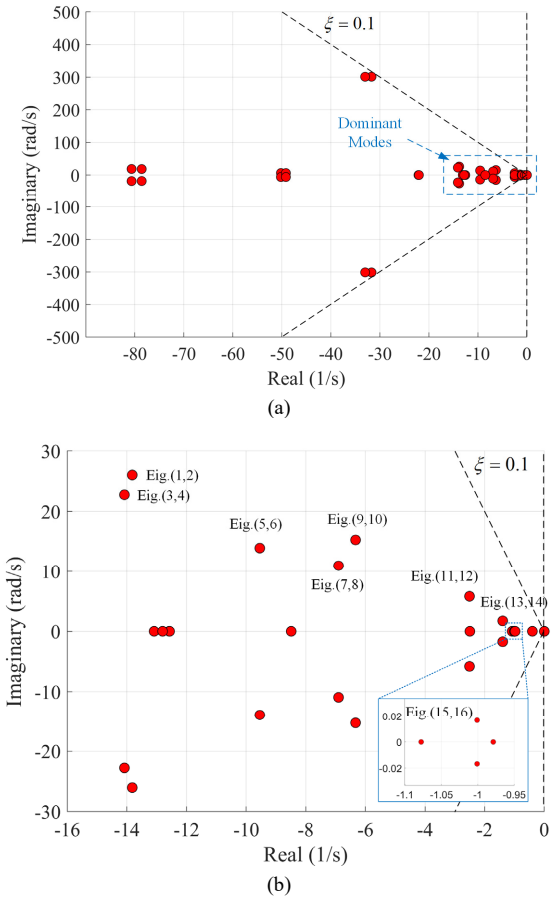

Fig. 5 (a). Overview modes of wind power-based microgrid. (b) Dominant modes of wind power-based microgrid.

oscillation modes should be greater than the specified value in order to ensure sufficient stability margin. Typically, the acceptable range of the damping ratio depends on the system sensitivity study and operational experience which is usually in the range of 0.03 to 0.05 for large and strong grid system [37]. In addition, due to the weak grid characteristics of the studied MG, it is recommended that the mid-low and ultra-low frequency oscillation modes should have better damping ratios that are greater than 0.1 [38]. A line with a damping ratio (ξ) of 0.1 can be seen in Fig. 5. All oscillation modes meet the requirements of the recommended damping ratio. In particular, the corresponding stator-rotor oscillation mode of the AGs can be found in Fig. 5 (a), which is also strongly associated with the state variables of Δi_{sdq} and Δi_{rdq}. The result in Fig. 5 reveals that it is able to obtain sufficient damping, which is different from the case of a single DFIG unit in Fig. 4.

3) Participation Factor Analysis

Participation factor can provide analysis on how the power generation units in MG create the oscillation modes. The modeling and eigenvalue analysis of wind power-based MG show that the dimension of the system described by state matrix A_{MG} is 73, while there are 29 pairs of complex-conjugate eigenvalues corresponding to 29 oscillation modes and appear 15 real negative eigenvalues. The participation matrix reflects the controllability and observability of the corresponding state

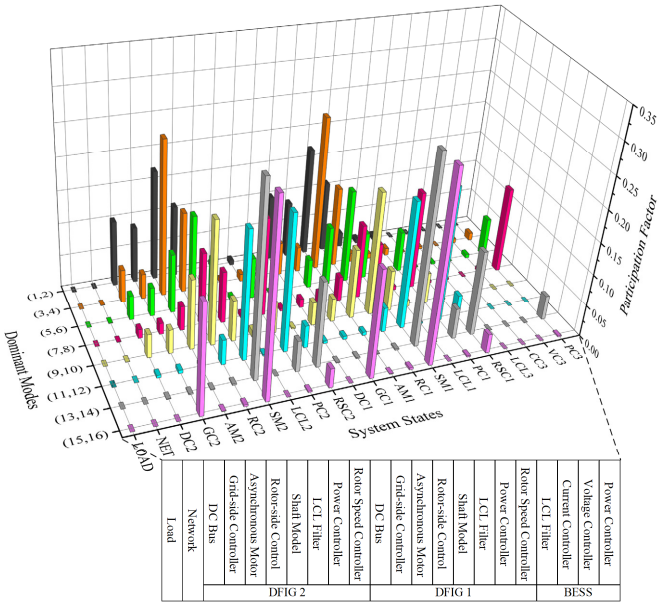

Fig. 6. Participation factor analysis of state variables of the system dominant modes.

variables in dominant modes. The participation factor analysis is carried out to figure out the correlation between state variables and oscillation modes.

Based on the dominant modes of the stability analysis, this section only considers eight pairs of eigenvalues of the dominant oscillation modes (i.e., Eigenvalues (1,2) - (15,16)). Fig. 6 presents the normalized system state variable participation factor in the system dominant modes.

Eigenvalues (1,2), (3,4), (5,6) and (9,10) represent the contributions of DFIG units because they are noticeably participated by the state variables of AG, RSC and GSC controller, as shown in Fig. 6. Eigenvalues (7,8) are dominated by the power controller of the three units and the RSC controller of the DFIG. The low-frequency Eigenvalues (11,12), (13,14) and the ultra-low frequency Eigenvalues (15,16) also represent the contributions of DFIG units because they are all affected by the state variables of the shaft model. Eigenvalues (11,12) are also dominated by the DFIGs' power controllers, (13,14) are also dominated by the rotor speed controllers and (15,16) are also a little affected by GSC controllers.

In summary, the wind turbines dominate the stability of the high-penetration wind power MG system. Secondly, the electromechanical transients of the DFIG shaft model directly lead to the weakly damping oscillations of ultra-low frequency in the MG. Although the proposed WPAD mechanism realizes the effective operation of the autonomous wind power-based MG, it leads to the mid-low frequency oscillation modes in the system. However, through effective parameter establishment and optimization, the damping of each oscillation mode can be successfully improved and stable operation of the system can be achieved.

4) Sensitivity Analysis

In order to further optimize the control parameters of the high-penetration wind power MG, the sensitivity analysis is studied. At the same time, this part can be mutually verified with

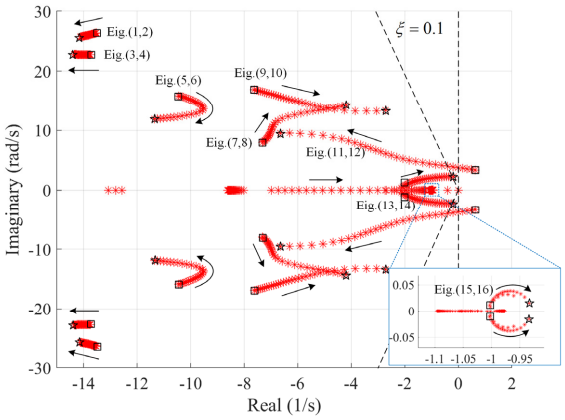

Fig. 7 Trajectory of dominant oscillatory modes when the crucial parameter K_{pwr} of rotor speed controller increases from $1e^{-3}$ to $3e^{-2}$ ($K_{iwr} = 3e^{-2}$).

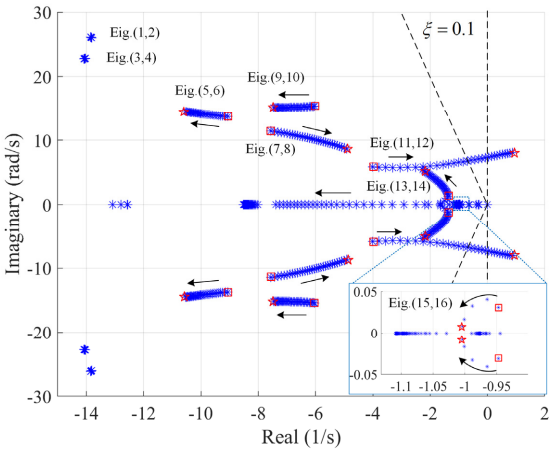

Fig. 8. Trajectory of dominant oscillatory modes when the crucial parameter K_{iwr} of rotor speed controller increases from $1e^{-3}$ to $15e^{-2}$ ($K_{pwr} = 1.5e^{-2}$).

participation factor analysis to figure out the key control parameters as well as improve the stability of the system.

Figs. 7 and 8 show the trajectory of dominant oscillatory modes when the proportional gain of the rotor speed controller K_{pwr} increases from $1e^{-3}$ to $3e^{-2}$ and integral gain of the rotor speed controller K_{iwr} increases from $1e^{-3}$ to $15e^{-2}$, respectively. As can be seen, the parameters of the rotor speed controller obviously cause the movement of Eigenvalues (7,8), (9,10), (11,12), (13,14). Among them, the Eigenvalues (11,12), (13,14) tend to move outside the damping line ($\xi = 0.1$), and even cross to the right half plane, which leads to system instability. This behavior also satisfies the conclusion of the participation factor analysis in Fig. 6. Because the parameters of the speed controller will affect the state variables of the power controller, it is consistent with the theoretical analysis that Eigenvalue (11,12) has a large moving range. Therefore, the proper value of K_{pwr} and K_{iwr} should be selected to ensure the sufficient damping ratio for low-frequency modes and the stability for the system.

Fig. 9 illustrates the eigenvalue loci of dominant modes for the active power droop coefficient m_p variations in the range of $5e^{-6}$ to $1e^{-4}$. It can be seen that the damping ratio of Eigenvalue

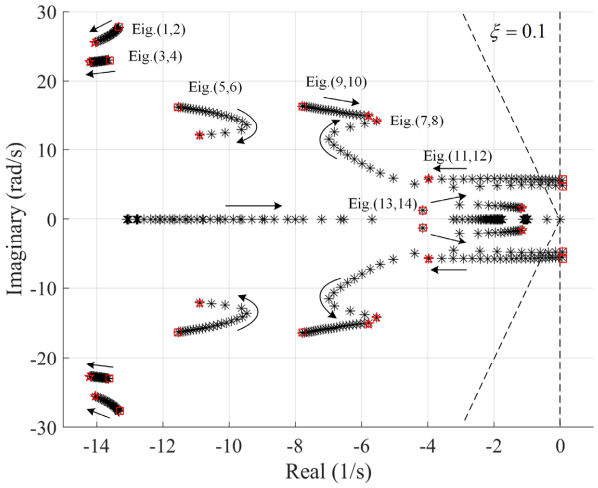

Fig. 9. Trajectory of dominant oscillatory modes when the crucial parameter m_p of power controller increases from $5e^{-6}$ to $1e^{-4}$.

(7,8) and (11,12) change obviously. And these dominant modes cross to the right half plane yielding oscillation responses. On the other hand, the dominant modes (7,8) and (11,12) in Fig. 6 are dominated by the power controller, further proving that the value of m_p will significantly change these two dominant modes.

Based on the above analysis, the parameters of the rotor speed controller and power controller are selected to be the critical control parameters, which can be optimized to the best value by participation factor analysis and sensitivity analysis for the following simulated and experimental verification. The optimized parameters are also given in Table II.

V. Simulation Results

In this section, in order to verify the effectiveness of the proposed decentralized grid-forming control strategy, a 30kVA DFIG-based MG is implemented under MATLAB/Simulink environment. Besides, the BESS operation scheme based on typical operating days is adopted for simulating the actual operating scenarios. Various testing scenarios are provided and analyzed in the following sections. It should be noted that this paper focuses on the design and analysis of decentralized grid-forming control strategy of high-penetration wind power MG in short-term time scale, and the following simulation results and analysis are based on the premise of the proposed typical operation. The optimal dispatch and operation of BESS in long-term time scale are beyond the scope of this paper.

A. BESS Operation Scheme Base on Typical Operating Days

As one of the units of the high-penetration wind power MG, the BESS applying grid-forming control strategy has the capability of power support and frequency regulation in the autonomous system. Cooperating with the MPPT function of DFIG, the BESS can reduce power output as much as possible to ensure economical operation under the heavy-load situation. Since the long-term time scale energy control dispatch problem is not the focus of this paper, in order to simplify the analysis of the BESS operation scheme, the typical operating day of the studied system is considered in this paper.

The variation of load power and wind power within typical

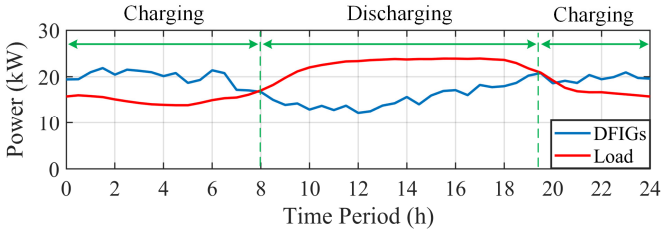

Fig. 10. Typical operating days scenario.

operating days is shown in Fig. 10. The load is larger than the wind power during daytime (about 8 a.m. to 7 p.m.) and the rest of the time at night is smaller than the wind power. Therefore, through the surplus and shortage of wind energy, the BESS is in charging and discharging state, respectively [39].

1) Charging Mode

It is possible and feasible to be in charging mode during load valley hours to store more power and transfer that to peak hours. When the BESS is in charging mode under the command of the MGCC, the DFIGs will operate at non-MPPT mode since only DFIGs can respond to load changes in the islanded MG system. At this time, the DFIGs are working in the adaptive droop area and the operating point of the DFIGs will adaptively move in the right half plane according to Fig. 2. It should be noted that the wind energy is sufficient for load and the charging power at night under the analysis of typical operating days. In addition, MGCC is able to calculate and update the charging power in real time, giving BESS charging commands.

2) Discharging Mode

It is necessary that the DFIGs operate in MPPT mode for maximum economical operation during BESS discharging state in daytime. Due to the wind power characteristic of anti-peak shaving, the maximum wind power captured is not enough for heavy-load thus the BESS is required to be involved for power support. It is noted that when the low-load situation occurs during the daytime, the BESS will shut down and transform into hot reservation mode. However, this scenario occurs rarely.

3) Discussion of the Impacts on BESS lifetime and economic

The lifetime of a BESS is usually quantified by the number of charging cycles, and the lifetime is mainly affected by frequent charging and discharging [40]. In the proposed control scheme of the studied system, MPPT as well as charge/discharge mode are the upper-level dispatch instructions from MGCC. Based on the typical operating days scenario, the BESS operation scheme achieves a charge-discharge cycle within 24 hours rather than charging/discharging frequently to compensate for the gaps between the load and wind power, which will severely shorten the lifetime of battery. In addition, whenever the wind energy is not sufficient for the load, the BESS participates in the power support, and at the same time, MPPT is activated according to the upper-level dispatch instructions. Therefore, the BESS unit operates in the most economical mode which can reduce power output as well as the charge-discharge cycles as much as possible. It should be pointed out that the quantitative analysis of BESS lifetime and

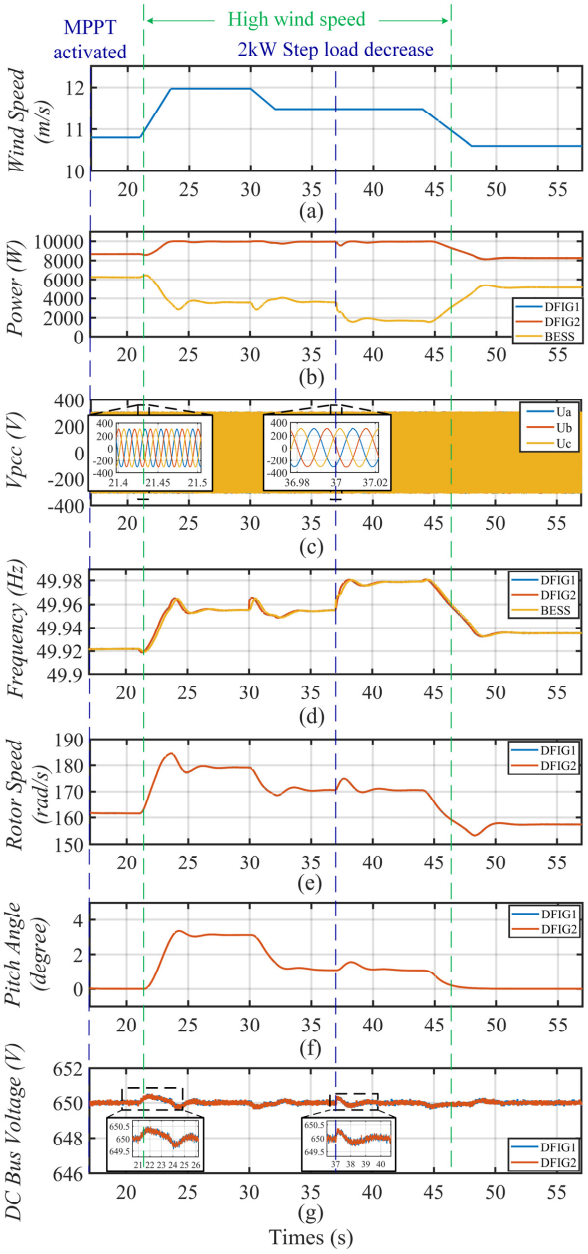

Fig. 11. System response of voltage-source wind power-based microgrid.

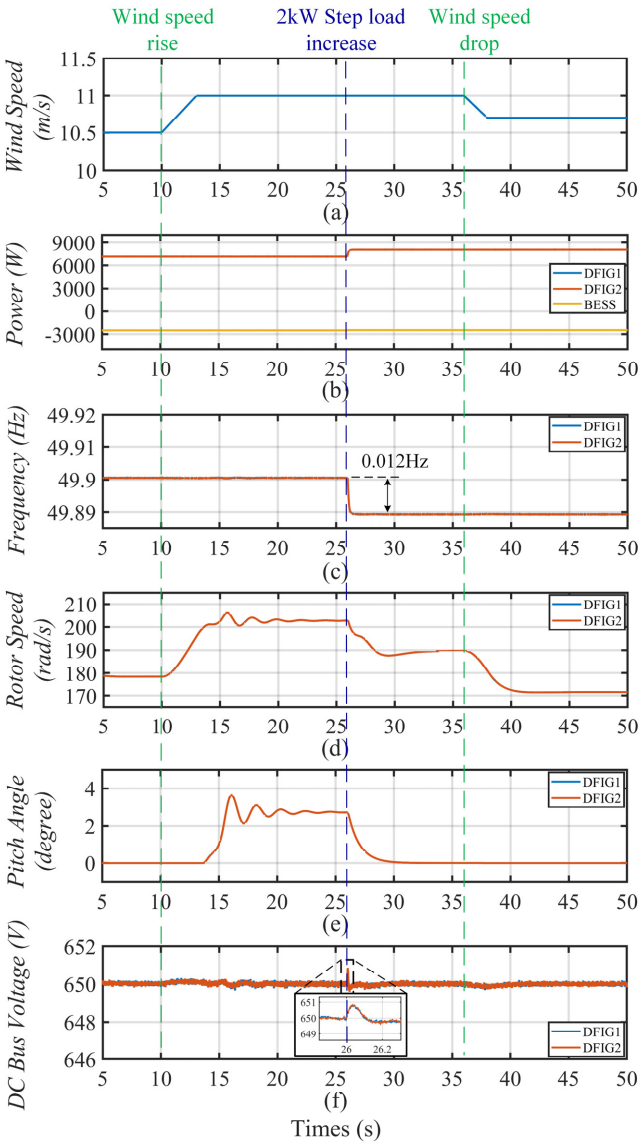

Fig. 12. System response of BESS charging state scenario.

economic is a long-term scheduling problem and it is beyond the scope of this paper.

B. Voltage-Source Operation of Wind Power-Based Microgrid

Fig. 11 presents the system response of the wind power-based MG when adopting the voltage-source WPAD control strategy. As can be seen, the MG carries a load and operates under a constant wind speed of 10.8 m/s. Since the two DFIGs are in MPPT mode, the remaining power is provided by BESS. Then, the wind speed gradually increased to 12 m/s, exceeding the nominal wind speed. The DFIGs quickly track to the maximum power output of 10 kW and the BESS reduces output power soon without fluctuation of the voltage at PCC during wind speed changes. Due to the wind speed rises, the rotor speed of DFIGs increases. The overspeed of the rotor causes the pitch angle to move and approach 3 degrees after stabilization shown in Fig. 11 (f), and the speed is stable within a safe range. The wind speed drops at t = 30 s but is still above the nominal wind speed and the DFIGs maintain the maximum power output. The rotor speed and pitch angle decreased and stabilized. When the step load decrease for 2 kW applied at t = 37 s, BESS reduces output power and the rotor speed and pitch angle maintain after transient changes. When the wind speed drops below the nominal wind speed, the rotor speed and pitch angle decrease resulting in more wind energy captured. The DC bus voltage is stable when the wind speed fluctuates and the load changes during the whole process as seen in Fig. 11 (g).

Although the DFIGs power is insufficient during the load peak hours, it is inevitable that a short-term high wind speed will occur at this time. It is worth mentioning that, since the DFIGs dominate the stability of the system; despite of the case of high wind speed in Fig. 11, the involved of the slower dynamic mechanical part does not affect the stability performance of the system.

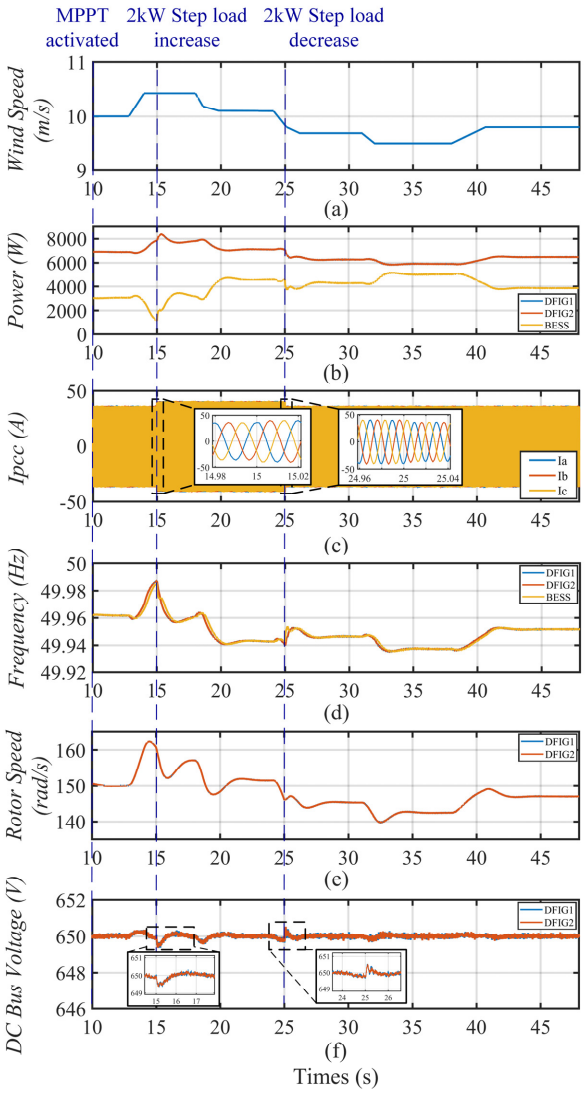

Fig. 13. System response under wind energy fluctuations.

C. BESS Charging State of Wind Power-Based Microgrid

The BESS is in charging mode during load valley hours to store more power which is shown in Fig. 12. Under the command of MGCC, the BESS is in a state of charge with a power of 2.5 kW, while the DFIGs are at non-MPPT mode in response to load changes in the autonomous MG system. Temporary changes in wind speed do not affect the power output of the DFIGs, but the rotor speed increases and overspeed causes pitch angle to move. At t = 26 s, a step load increase of 2 kW is applied and each DFIG increases the output power for 1 kW since the droop coefficients are the same. As seen in Fig. 12 (d) and (e), when the step load is applied, the kinetic energy of the rotors is released in exchange for the system power, and the rotor speed decreases as well as the pitch angle in order to capture more wind energy. According to the designed droop curve, the output frequency decreases by 0.012 Hz under load changes shown in Fig. 12 (c), which is not a wide range of deviation and is acceptable for operation. In conclusion, the system can also have satisfactory stability and excellent dynamic performance in the charging state.

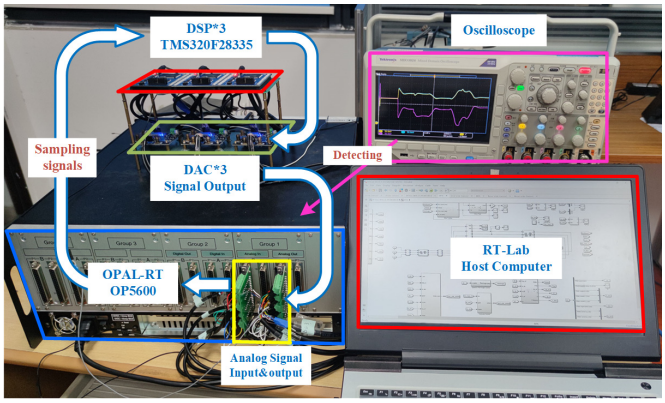

Fig. 14. Hardware-in-the-loop experimental environment framework.

D. Wind Speed Fluctuations Scenarios of Wind Power-Based Microgrid

In order to ensure the satisfactory performance of the wind power-based system in the presence of wind energy fluctuations, the system response should be examined under continuous wind speed volatility. Fig. 13 presents the system dynamic when wind speed is continuously increased and decreased after activation of voltage-source MPPT of DFIGs. As can be seen, the system carries a load of 17 kW and starts to operate in MPPT mode under a wind speed of 10 m/s. All units are initially enabled to operate stably and then wind speed increase to 10.43 m/s. ω_r^{ref} can be dynamically updated and calculated by the MPPT controller, rotor speed can quickly track the reference speed. A step load increase and decrease of 2kW applied in t = 15 s and 20s, respectively. As shown in Fig. 13 (c), the current of PCC has a step change but achieves low total harmonic distortion during operation. The output power and frequency of the system can be adaptively regulated through the WPAD mechanism, as shown in Figs. 13 (b) and (d).

In conclusion, the situation of reduced wind energy accompanied by the load transition can also have satisfactory performance, which is in accordance with the actual operation. In spite of the load transition and variable operating conditions, the response of the system is still in line with expectations.

VI. Hardware in the Loop Experimental Results

A. Hardware-in-the-Loop Experimental Setup

As shown in Fig. 14, RT-Lab is used to execute the model in real-time simulator OPAL-RT OP5600. It is worth noting that, according to the above analysis, the WPAD control loop is the strategy that determines the system control target. Therefore, the WPAD control loops in Fig. 3 of the three units are executed in DSP hardware (TMS320F28335). The main circuit system as well as the mechanical components are implemented in the real-time simulator. And the remaining voltage and current control loops are also implemented in the real-time simulator, since the remaining loops can be regarded as fast dynamics that do not dominate the system dynamics.

The experimental environment also includes the host computers and three DAC signal output modules shown in Fig. 14. A set of DSP and DAC composes a WPAD control strategy

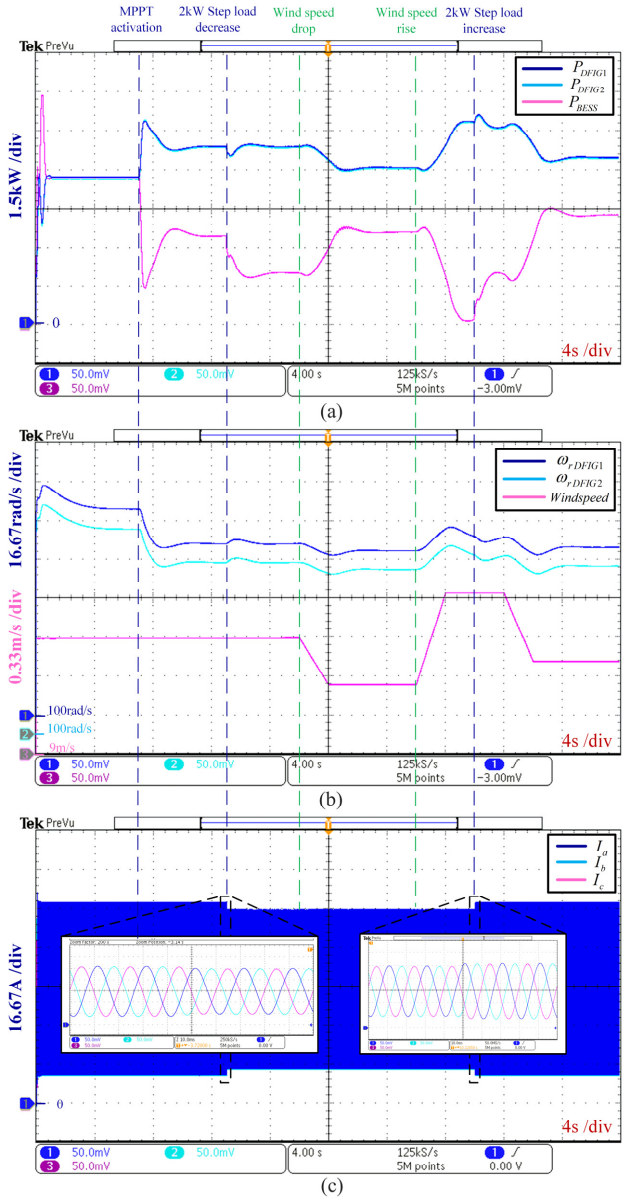

Fig. 15. System response under typical operation conditions of HIL experiment. (a) Output active power of three units. (b) Rotor speed of DFIG units and wind speed. (c) Output current of PCC.

for one unit. DSPs collect analog signals from RT-Lab, and after completing the control strategy calculation, they cooperate with DACs to transmit the signals back to RT-Lab. Thus, HIL experimental environment is setup.

B. Experiment of High-Penetration Wind Power Microgrid under Typical Operation Conditions

To demonstrate the dynamic response of the system, the typical operation conditions are selected for experimental verification. Fig. 15 (a) shows the HIL experiment results of the output power of three units in the studied MG system. The system carries a load of 17kW under a wind speed of 10m/s. The successful activation of MPPT demonstrates the feasibility of the WPAD mechanism operated in the actual hardware control loop. Under the control of the rotor speed controller, the rotor speed is kept within a reasonable range even if the wind speed and load disturbance. The current of the PCC determined by the load has a step change but has low total harmonic distortion during operation. As shown in Fig. 15, the performance of the system is satisfactory in the context of load transition and wind energy fluctuations, which can simulate the most realistic and typical operation scenario. This verifies the effectiveness of the proposed WPAD scheme in flexible power regulation for autonomous microgrid operation.

VII. Conclusion

This paper addressed the overall control and dynamic interactions of the high-penetration wind power microgrid. A decentralized grid-forming strategy of wind power-based MG without PLL is proposed, cooperating with the implementation of wind power adaptive dynamic droop control mechanism, achieving the effect of reasonable power distribution and economical operation in the system. A detailed full-order state-space model of the studied microgrid system considering electromechanical transients of the mechanical components and adaptive droop control mechanism is developed. Small-signal stability analysis reveals that WTGs dominate the stability of the wind power-based microgrid system. Moreover, the proposed WPAD mechanism and the DFIG electromechanical transients directly lead to the weakly damping oscillation modes of mid-low and ultra-low frequency, respectively. Through effective parameters selection, the damping of each oscillation mode is improved and system stability is enhanced significantly. In order to verify the feasibility of the proposed framework, time-domain simulation results under various scenarios are presented to realize the effective operation of the wind power-based system. Furthermore, hardware-in-the-loop experiments under typical operation conditions further verify the effectiveness of the proposed scheme to achieve the control target in actual operation.

References

[1] S. Eftekharnejad, V. Vittal, G. T. Heydt, B. Keel and J. Loehr, "Impact of increased penetration of photovoltaic generation on power systems," *IEEE Transactions on Power Systems*, vol. 28, no. 2, pp. 893-901, May 2013.

[2] N. Gupta, "Probabilistic Optimal Reactive Power Planning With Onshore and Offshore Wind Generation, EV, and PV Uncertainties," *IEEE Transactions on Industry Applications*, vol. 56, no. 4, pp. 4200-4213, July-Aug. 2020.

[3] S. Kumar Tiwari, B. Singh and P. K. Goel, "Design and Control of Microgrid Fed by Renewable Energy Generating Sources," *IEEE Transactions on Industry Applications*, vol. 54, no. 3, pp. 2041-2050, May-June 2018.

[4] M. Fazeli, G. M. Asher, C. Klumpner, L. Yao and M. Bazargan, "Novel Integration of Wind Generator-Energy Storage Systems Within Microgrids," *IEEE Transactions on Smart Grid*, vol. 3, no. 2, pp. 728-737, June 2012.

[5] Viktor Sebestyén, "Renewable and Sustainable Energy Reviews: Environmental impact networks of renewable energy power plants," *Renewable and Sustainable Energy Reviews*, vol. 151, 111626, Nov. 2021.

[6] J. Rocabert, A. Luna, F. Blaabjerg and P. Rodríguez, "Control of Power Converters in AC Microgrids," *IEEE Transactions on Power Electronics*, vol. 27, no. 11, pp. 4734-4749, Nov. 2012.

[7] K. V. Vidyanandan and N. Senroy, "Primary frequency regulation by deloaded wind turbines using variable droop," *IEEE Transactions on Power Systems*, vol. 28, no. 2, pp. 837-846, May 2013.

[8] L. Holdsworth, J. B. Ekanayake, and N. Jenkins, "Power system frequency response from fixed speed and doubly fed induction generator-based wind turbines," *Wind Energy*, vol. 7, no. 1, pp. 21–35, 2004.

[9] S. Ghosh, S. Kamalasadan, N. Senroy and J. Enslin, "Doubly Fed Induction Generator (DFIG)-Based Wind Farm Control Framework for Primary Frequency and Inertial Response Application," *IEEE Transactions on Power Systems*, vol. 31, no. 3, pp. 1861-1871, May 2016.
[10] M. Fakhari Moghaddam Arani and Y. A. I. Mohamed, "Dynamic Droop Control for Wind Turbines Participating in Primary Frequency Regulation in Microgrids," *IEEE Transactions on Smart Grid*, vol. 9, no. 6, pp. 5742-5751, Nov. 2018.
[11] J. Morren, S. W. H. de Haan, W. L. Kling and J. A. Ferreira, "Wind turbines emulating inertia and supporting primary frequency control," *IEEE Transactions on Power Systems*, vol. 21, no. 1, pp. 433-434, Feb. 2006.
[12] Z. Xie, Y. Feng, M. Ma and X. Zhang, "An Improved Virtual Inertia Control Strategy of DFIG-Based Wind Turbines for Grid Frequency Support," *IEEE Journal of Emerging and Selected Topics in Power Electronics*, vol. 9, no. 5, pp. 5465-5477, Oct. 2021.
[13] M. F. M. Arani and E. F. El-Saadany, "Implementing Virtual Inertia in DFIG-Based Wind Power Generation," *IEEE Transactions on Power Systems*, vol. 28, no. 2, pp. 1373-1384, May 2013.
[14] Y. Tan, L. Meegahapola and K. M. Muttaqi, "A Suboptimal Power-Point-Tracking-Based Primary Frequency Response Strategy for DFIGs in Hybrid Remote Area Power Supply Systems," *IEEE Transactions on Energy Conversion*, vol. 31, no. 1, pp. 93-105, March 2016.
[15] C. Wang, J. Li and Y. Hu, "Frequency Control of Isolated Wind-Diesel Microgrid Power System by Double Equivalent-Input-Disturbance Controllers," *IEEE Access*, vol. 7, pp. 105617-105626, 2019.
[16] N. T. Janssen, R. W. Wies and R. A. Peterson, "Frequency Regulation by Distributed Secondary Loads on Islanded Wind-Powered Microgrids," *IEEE Transactions on Sustainable Energy*, vol. 7, no. 3, pp. 1028-1035, July 2016.
[17] C. Liang, P. Wang, X. Han, W. Qin, Y. Jia and T. Yuan, "Battery Energy Storage Selection Based on a Novel Intermittent Wind Speed Model for Improving Power System Dynamic Reliability," *IEEE Transactions on Smart Grid*, vol. 9, no. 6, pp. 6084-6094, Nov. 2018.
[18] Z. Zhao, P. Yang, Y. Wang, Z. Xu and J. M. Guerrero, "Dynamic Characteristics Analysis and Stabilization of PV-Based Multiple Microgrid Clusters," *IEEE Transactions on Smart Grid*, vol. 10, no. 1, pp. 805-818, Jan. 2019.
[19] H. Xiao, Z. Zhao, K. Zhou, J. Guo, C. S. Lai and L. Lei Lai, "Voltage-Source Control of DFIG in Standalone Wind Power-Based Microgrids," *2020 IEEE 1st China International Youth Conference on Electrical Engineering (CIYCEE)*, 2020, pp. 1-7.
[20] Yuan, X. , and Y. Li . "Control of variable pitch and variable speed direct-drive wind turbines in weak grid systems with active power balance." *Iet Renewable Power Generation*, vol. 8, no. 2, pp. 119-131, 2014.
[21] Y. Tang, Z. Zhang and Z. Xu, "DRU Based Low Frequency AC Transmission Scheme for Offshore Wind Farm Integration," *IEEE Transactions on Sustainable Energy*, vol. 12, no. 3, pp. 1512-1524, July 2021.
[22] W. Yan, L. Cheng, S. Yan, W. Gao and D. W. Gao, "Enabling and Evaluation of Inertial Control for PMSG-WTG Using Synchronverter With Multiple Virtual Rotating Masses in Microgrid," *IEEE Transactions on Sustainable Energy*, vol. 11, no. 2, pp. 1078-1088, April 2020.
[23] A. Bidadfar, O. Saborío-Romano, N. A. Cutululis and P. E. Sørensen, "Control of Offshore Wind Turbines Connected to Diode-Rectifier-Based HVdc Systems," *IEEE Transactions on Sustainable Energy*, vol. 12, no. 1, pp. 514-523, Jan. 2021.
[24] Y. Jiao and H. Nian, "Grid-Forming Control for DFIG Based Wind Farms to Enhance the Stability of LCC-HVDC," *IEEE Access*, vol. 8, pp. 156752-156762, 2020.
[25] H. Nian and Y. Jiao, "Improved Virtual Synchronous Generator Control of DFIG to Ride-Through Symmetrical Voltage Fault," *IEEE Transactions on Energy Conversion*, vol. 35, no. 2, pp. 672-683, June 2020.
[26] M. Rasheduzzaman, J. A. Mueller and J. W. Kimball, "An Accurate Small-Signal Model of Inverter- Dominated Islanded Microgrids Using dq Reference Frame," *IEEE Journal of Emerging and Selected Topics in Power Electronics*, vol. 2, no. 4, pp. 1070-1080, Dec. 2014.
[27] R. Wang, Q. Sun, D. Ma and Z. Liu, "The Small-Signal Stability Analysis of the Droop-Controlled Converter in Electromagnetic Timescale," *IEEE Transactions on Sustainable Energy*, vol. 10, no. 3, pp. 1459-1469, July 2019.
[28] N. Pogaku, M. Prodanovic and T. C. Green, "Modeling, Analysis and Testing of Autonomous Operation of an Inverter-Based Microgrid," *IEEE Transactions on Power Electronics*, vol. 22, no. 2, pp. 613-625, March 2007.
[29] A. Aderibole, H. H. Zeineldin and M. Al Hosani, "A Critical Assessment of Oscillatory Modes in Multi-Microgrids Comprising of Synchronous and Inverter-Based Distributed Generation," *IEEE Transactions on Smart Grid*, vol. 10, no. 3, pp. 3320-3330, May 2019.
[30] M. F. M. Arani and Y. A. I. Mohamed, "Analysis and Impacts of Implementing Droop Control in DFIG-Based Wind Turbines on Microgrid/Weak-Grid Stability," *IEEE Transactions on Power Systems*, vol. 30, no. 1, pp. 385-396, Jan. 2015.
[31] Z. Zhao, P. Yang, J. M. Guerrero, Z. Xu and T. C. Green, "Multiple-Time-Scales Hierarchical Frequency Stability Control Strategy of Medium-Voltage Isolated Microgrid," *IEEE Transactions on Power Electronics*, vol. 31, no. 8, pp. 5974-5991, Aug. 2016.
[32] B. Qian, Z. Liu, J. Fang, X. Liu and L. Zhang, "The Study of Sliding Mode Control Strategy for Luxi Island Micro-grid," *2018 2nd IEEE Advanced Information Management, Communicates, Electronic and Automation Control Conference (IMCEC)*, 2018, pp. 1762-1766.
[33] W. Du, Q. Jiang, M. J. Erickson and R. H. Lasseter, "Voltage-Source Control of PV Inverter in a CERTS Microgrid," *IEEE Transactions on Power Delivery*, vol. 29, no. 4, pp. 1726-1734, Aug. 2014.
[34] F. Mei and B. Pal, "Modal Analysis of Grid-Connected Doubly Fed Induction Generators," *IEEE Transactions on Energy Conversion*, vol. 22, no. 3, pp. 728-736, Sept. 2007.
[35] L. P. Kunjumuhammed, B. C. Pal, C. Oates and K. J. Dyke, "Electrical Oscillations in Wind Farm Systems: Analysis and Insight Based on Detailed Modeling," *IEEE Transactions on Sustainable Energy*, vol. 7, no. 1, pp. 51-62, Jan. 2016
[36] Y. Peng, Z. Shuai, L. Che, M. Lyu and Z. J. Shen, "Dynamic Stability Improvement and Accurate Power Regulation of Single-Phase Virtual Oscillator Based Microgrids," *IEEE Transactions on Sustainable Energy*, vol. 13, no. 1, pp. 277-289, Jan. 2022.
[37] R. Farmer, "Power systems dynamics and stability," *The Electric Power Engineering Handbook*, L. Grigsby, Ed. Boca Raton, FL, USA: CRC Press, 2001.
[38] B. Pal and B. Chaudhuri, *Robust Control in Power Systems*. New York, NY, USA: Springer, 2005.
[39] F. Luo, K. Meng, Z. Y. Dong, Y. Zheng, Y. Chen and K. P. Wong, "Coordinated Operational Planning for Wind Farm with Battery Energy Storage System," *IEEE Transactions on Sustainable Energy*, vol. 6, no. 1, pp. 253-262, Jan. 2015.
[40] Y. Zheng, Z. Y. Dong, F. J. Luo, K. Meng, J. Qiu and K. P. Wong, "Optimal Allocation of Energy Storage System for Risk Mitigation of DISCOs with High Renewable Penetrations," *IEEE Transactions on Power Systems*, vol. 29, no. 1, pp. 212-220, Jan. 2014.

Zhuoli Zhao (S'15–M'18) received the Ph.D. degree in electrical engineering from South China University of Technology, Guangzhou, China, in 2017. From October 2014 to December 2015, he was a Joint Ph.D. Student and Sponsored Researcher with the Control and Power Research Group, Department of Electrical and Electronic Engineering, Imperial College London, London, U.K. He was a Research Associate with the Smart Grid Research Laboratory, Electric Power Research Institute, China Southern Power Grid, Guangzhou, China, from 2017 to 2018.

He is currently an Associate Professor with the School of Automation, Guangdong University of Technology, Guangzhou, China. His research interests include microgrid control and energy management, renewable power generation control and grid-connected operation, modeling, analysis and control of power-electronized power systems and smart grids. He is an Associate Editor of the Protection and Control of Modern Power Systems (PCMP). He is an Active Reviewer for the IEEE Transactions on Smart Grid, the IEEE Transactions on Sustainable Energy, the IEEE Transactions on Industrial Electronics, the IEEE Transactions on Power Electronics, and the Applied Energy.

Xi Luo received the B.E. degree from Guangdong University of Technology, Guangzhou, China, in 2020. He is currently working toward the master degree in electrical engineering with the School of Automation, Guangdong University of Technology, Guangzhou, China. His research interests include microgrid control and operation.

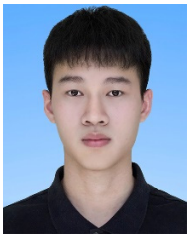

Jindian Xie received the B.E. degree from Dongguan University of Technology, Dongguan, China, in 2020. He is currently working toward the master degree in electrical engineering with the School of Automation, Guangdong University of Technology, Guangzhou, China. His research interests include the stability analysis and control of microgrid.

Shaoqing Gong received the B.E. degree in electrical engineering from Changchun University of Science and technology, Changchun, China, in 2020. He is currently studying for a master's degree from Guangdong University of Technology, Guangzhou, China. His current research interests include microgrid, renewable energy system, model predictive control.

Juntao Guo received the B.E. degree from Guangdong University of Technology, Guangzhou, China, in 2019. He is currently working toward the master degree in electrical engineering with the School of Automation, Guangdong University of Technology, Guangzhou, China. His research interests include microgrid control and energy management.

Qiang Ni received the M.Sc. and Ph.D. degrees in electrical engineering from Southwest Jiaotong University, Chengdu, China, in 2013 and 2018, respectively.

He is currently a Lecturer with the Guangdong University of Technology, Guangzhou, China. His research interests include forecasting and control technology for multi-energy system, intelligent fault diagnosis and health management of the power electronic system.

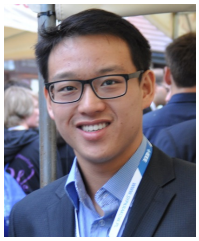

Chun Sing Lai (S'11, M'19, SM'20) received the B.Eng. (First Class Hons.) in electrical and electronic engineering from Brunel University London, London, UK, in 2013, and the D.Phil. degree in engineering science from the University of Oxford, Oxford, UK, in 2019.

He is currently a Lecturer with the Department of Electronic and Electrical Engineering, Brunel University London. From 2018 to 2020, he was an UK Engineering and Physical Sciences Research Council Research Fellow with the School of Civil Engineering, University of Leeds, Leeds, UK. His current research interests are in power system optimization and data analytics. Dr. Lai was the Publications Co-Chair for both 2020 and 2021 IEEE International Smart Cities Conferences. He is the Vice-Chair of the IEEE Smart Cities Publications Committee and Associate Editor for IET Energy Conversion and Economics. He is the Working Group Chair for IEEE P2814 Standard, an Associate Vice President, Systems Science and Engineering of the IEEE Systems, Man, and Cybernetics Society (IEEE/SMCS) and the Chair of the IEEE SMC Intelligent Power and Energy Systems Technical Committee. He is an IET Member and a Chartered Engineer.

Ping Yang (M'11) received the Ph.D. degree in automatic control from South China University of Technology, Guangzhou, China, in 1998. She is currently a Professor with the School of Electric Power Engineering, South China University of Technology, Guangzhou, China and the Director of Guangdong Key Laboratory of Clean Energy Technology, South China University of Technology, Guangzhou, China. Her current research interests include smart microgrid and electricity market.

Loi Lei Lai (M'87, SM'92, F'07, LF'21) received the B.Sc. (First Class Hons.), Ph.D., and D.Sc. degrees in electrical and electronic engineering from the University of Aston, Birmingham, UK, and City, University of London, London, UK, in 1980, 1984, and 2005, respectively.

Professor Lai is currently a University Distinguished Professor with Guangdong University of Technology, Guangzhou, China. He was a Pao Yue Kong Chair Professor with Zhejiang University, Hangzhou, China, and the Professor and Chair of Electrical Engineering with City, University of London. His current research areas are in smart cities and smart grid. Professor Lai was awarded an IEEE Third Millennium Medal, the IEEE Power and Energy Society (IEEE/PES) UKRI Power Chapter Outstanding Engineer Award in 2000, the IEEE/PES Energy Development and Power Generation Committee Prize Paper in 2006 and 2009, the IEEE Systems, Man, and Cybernetics

Society (IEEE/SMCS) Outstanding Contribution Award in 2013 and 2014, the Most Active Technical Committee Award in 2016, and his research team has received a Best Paper Award in the IEEE International Smart Cities Conference in October 2020. Professor Lai is an Associate Editor of the IEEE Transactions on Systems, Man, and Cybernetics: Systems, Editor-in-Chief of the IEEE Smart Cities Newsletter, a member of the IEEE Smart Cities Steering Committee and the Chair of IEEE/SMCS Standards Committee. He was a member of the IEEE Smart Grid Steering Committee; the Director of Research and Development Center, State Grid Energy Research Institute, China; a Vice President for Membership and Student Activities of IEEE/SMCS; and a Fellow Committee Evaluator for the IEEE Industrial Electronics Society. He is a Fellow of IET.

Josep M. Guerrero (S'01-M'04-SM'08-F'15) received the B.Sc. degree in telecommunications engineering, the M.Sc. degree in electronics engineering, and the Ph.D. degree in power electronics from the Technical University of Catalonia, Barcelona, in 1997, 2000 and 2003, respectively. Nowadays he is working towards the M.Sc. Degree in Psychobiology and Cognitive Neuroscience at the Autonomous University of Barcelona.

Since 2011, he has been a Full Professor with AAU Energy, Aalborg University, Denmark, where he is responsible for the Microgrid Research Program. From 2019, he became a Villum Investigator by The Villum Fonden, which supports the Center for Research on Microgrids (CROM) at Aalborg University, being Prof. Guerrero the founder and Director of the same center (www.crom.et.aau.dk).

His research interests is oriented to different microgrid frameworks in applications like microgrid clusters, IoT-based and digital twin, maritime microgrids for electrical ships, vessels, ferries and seaports, and space microgrids applied to nanosatellites and closed ecological systems. Prof. Guerrero is an Associate Editor for a number of IEEE TRANSACTIONS. He has published more than 800 journal papers in the fields of microgrids and renewable energy systems, which are cited more than 70,000 times. During eight consecutive years, from 2014 to 2021, he was awarded by Clarivate Analytics (former Thomson Reuters) as Highly Cited Researcher with 50 highly cited papers. In 2021, he received the IEEE Bimal Bose Award for Industrial Electronics Applications in Energy Systems, for his pioneering contributions to renewable energy based microgrids.